Directed percolation front in a gradient

1991 J. Phys. A: Math. Gen. 24 1611

(http://iopscience.iop.org/0305-4470/24/7/032)

J. Phys. A: Math. Gen. 24 (1991) 1611-1623. Printed in the UK

Directed percolation front in a gradient

Stéphane Roux†§ and Etienne Guyon‡§

† Centre d'Enseignement et de Recherche en Analyse des Matériaux, Ecole Nationale des Ponts et Chaussées, Central IV, 1 Avenue Montaigne, F-93167 Noisy-le-Grand Cédex, France

‡ Palais de la Découverte, Avenue Franklin Roosevelt, F-75016 Paris, France

Received 12 October 1990

Abstract. We study numerically the structure of fronts generated in a directed percolation problem in two dimensions when the probability for a bond to be present decreases linearly along one direction. We discuss several cases of relative orientation of the preferential direction with respect to the gradient. We also consider the Domany-Kinzel limit case of directed percolation, and obtain analytical results. The structure of the front is analysed using the jump size distribution introduced by Hansen *et al.*

1. Introduction

There has been recently a large number of studies devoted to the structure of fronts in various physical systems where disorder is important. Among these we can mention percolation fronts in a gradient [2, 3], rain model fronts (ballistic deposition of particles) [4-6], surface of Eden clusters [7-9] etc. The scaling properties of the front have been obtained numerically, or theoretically in some cases.

We propose in this article to study the geometrical structure of fronts appearing in a directed percolation process in a gradient. This model can be related to previous front models in the case of an extreme disorder. The results obtained for directed percolation at threshold, and the one relative to percolation in a gradient seem *a priori* sufficient to understand completely the scaling properties. We will see however that, despite the apparent simplicity of the problem, some scaling exponents cannot simply be related to the classical properties of directed percolation with no gradient.

Other motivations for studying this problem can be found in the usual applications [10] of directed percolation, e.g. chemical reactions, contamination models, cellular automata, forest fires, ... with an overall variation of the control parameter. When the preferential direction is considered as being a 'time' parameter, the gradient we consider is either a temporal decrease of the presence probability (hereafter model A), or a spatial inhomogeneity (models B, C and D). A last reason is the accurate determination of a critical control parameter (threshold) for a directed process, and possible comparison with known cases to identify a universality class. This was the case in [1], where Hansen *et al* studied a model similar to one of those we will consider. We will

§ Also at Laboratoire de Physique et Mécanique des Milieux Hétérogènes, URA CNRS 857, Ecole Supérieure de Physique et Chimie Industrielles, 10 rue Vauquelin, F-75231 Paris Cédex 05, France.

0305-4470/91/071611+13$03.50

follow the analysis they propose, i.e. studying the jump height distribution in order to get some insight in the front structure.

2. Presentation of the problem

Let us consider a strip-shaped square lattice whose principal axis forms a $\pi/4$ angle with the length of the strip as shown in figure 1. The bonds in the lattice are present with a probability that varies linearly along the width. At a distance y from a border (labelled S in figure 1), the probability that a bond is present is $p(y) = 1 - y/w$ where w is the width of the strip. Thus the bonds touching S are all present ($p(0) = 1$), whereas those on the opposite border are all absent ($p(w) = 0$). The gradient of probability will always keep the same orientation in all the cases we will consider hereafter. In figure 1, we indicate the direction of the gradient with an arrow labelled G. Now, we select a 'preferential direction' along one diagonal of the square lattice, i.e. we define an orientation of the two principal axes of the lattice. Figure 1 shows these directions for various examples with the arrows labelled D.

Starting from the border S of the strip, we define the cluster of sites which can be reached by a *directed* walk through present bonds, always moving along the preferential direction chosen previously. Since no bond can be present along the facing border where $p = 0$, obviously the cluster will be confined strictly inside the strip. We now probe the front of this cluster in a test direction T (shown in figure 1) by looking for the first site of the cluster one encounters by moving along one axis of the square lattice and starting from the border where no bond is present. This set of sites forms the front of the cluster. By construction, this front will depend on the three directions G, D and T. Figure 1(a-c) shows the relative orientations chosen in three cases which will be referred to as A, B and C in the following. We will study numerically the structure of the front in these three cases. Let us note that B and C only differ by the relative orientation of the test direction 'T'.

Finally, we will complement our study with a solvable case, shown in figure 1(d). Domany and Kinzel [11] have considered a limit case of directed percolation which can be solved exactly: along one axis of the square lattice *all bonds* are present. When the probability for having a bond present along the other axis is uniform in space, one can map this directed percolation onto a random walk problem, and thus solve it exactly. We will show that we can study the structure of the front when a gradient of probability is introduced in the model. Figure 1(d) shows the only relative orientation of G and D which gives rise to a non-degenerated front. Let us, however, stress that the universality class of the Domany-Kinzel problem is different from the usual directed percolation case [11].

3. Numerical simulations

In all cases, A, B and C, we performed similar computations. Since information can only propagate along the preferential direction, it suffices to keep in memory the status of the sites located on a section of the strip (along the T direction). By status we mean whether the site is part of the cluster or not. The principle of the computation is simply to compute the status of the sites located on the next section of the strip, and reiterate. The resulting section is then used as the starting condition for the rest of the computation

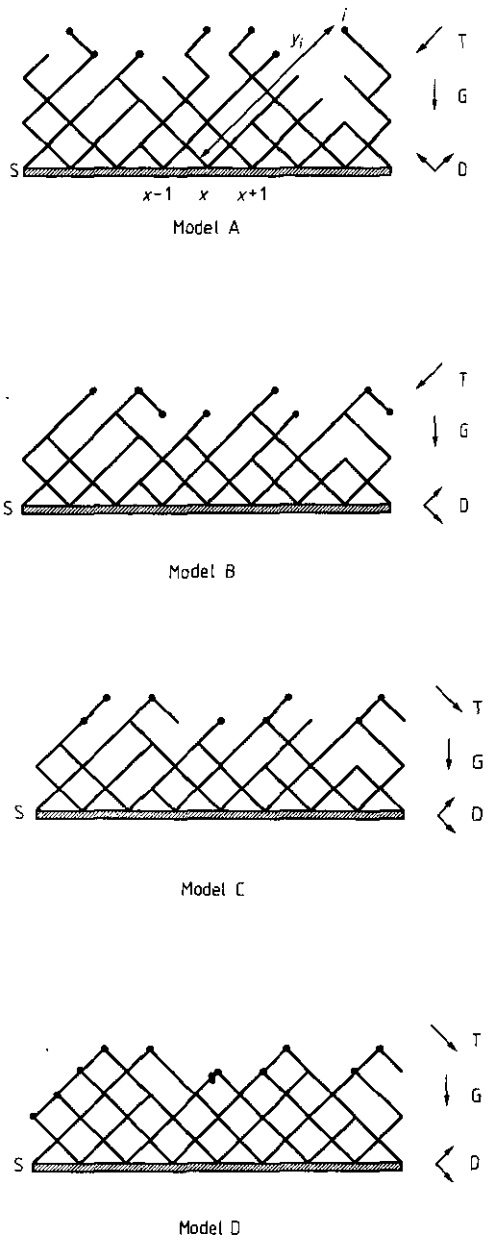

Figure 1. The four different models studied in this article. All bonds are present close to the lower border of the strip, S. The presence probability decreases linearly with the distance to S. The arrows G indicate the direction of the gradient of probability. All bonds are oriented by the arrows labelled D. The position of the front is characterized in each row parallel to T by the top site one can reach with a directed walk starting from S. Cases A, B and C differ by the relative orientation of G, D and T. In case D, all bonds are present in one direction (north-east). The dots on the figures represent the top sites (such as i) in each row labelled by x. The distance from this site to the S border is called y and is shown for model A for site i.

where all necessary information about the structure of the front is recorded. The length of the strip was chosen to be 10^5 in all cases (for all values of the gradient and all models). At the start of the computation, the first section has only one site which belongs to the cluster (the site which is on the S border). In order to get rid of edge effects due to this initial state, we first generate a length of strip equal to ten times its width before recording the data.

We mentioned in the introduction that the probability to have a bond present was $p(y) = 1 - y/w$. However, since the front is generally confined to a narrow region close to $p(y) = p_c$, a large part of the strip is useless. Therefore, in practice, we restricted the variation of $p(y)$ between two extreme values $p_{min} \leqslant p \leqslant p_{max}$, chosen such that the front never reaches the borders. The gradient $g = -dp(y)/dy$ ranged from 2×10^{-2} to 10^{-4}. For $g = 10^{-4}$ the effective width of the strip was 10^3 (and not 10^4 as would have been necessary if $0 \leqslant p \leqslant 1$). We checked that the front never reaches the two borders, so that the restricted range $p_{min} \leqslant p \leqslant p_{max}$ did not affect the structure of the front. In the rest of the paper we will, however, refer to the width of the strip that would be necessary for p to range from zero to one, or equivalently $w = 1/g$.

4. Results

By probing the front along lines parallel to T, we get one site i per section. We recorded the distance y_i from this site to the border S, by simply counting the number of bonds needed to reach i from S. The mean distance from the front to the border S is

$$\langle y \rangle = (1/L) \sum_i y_i \tag{1}$$

where L is the length of the strip. For long enough strips, $\langle y \rangle$ does not depend on L, but only on the gradient g. The width of the front, z, can simply be estimated by the fluctuation of y_i:

$$z^2 = \langle y^2 \rangle - \langle y \rangle^2. \tag{2}$$

Rather than using the distance, we translate the above quantities into the corresponding probabilities, using the linearity of $p(y)$: The mean distance $\langle y \rangle$ corresponds to a mean probability $P(g)$, and the width z corresponds to a fluctuation $\sigma(g)$:

$$P(g) = p(\langle y \rangle) \qquad \sigma(g) = gz. \tag{3}$$

In models A, B and C, $P(g)$ converges when the gradient tends to zero to the directed percolation threshold on the square lattice. One of the most precise determination of this threshold is $p_c = 0.644701 \pm 1 \times 10^{-6}$ found in [12]. The convergence of $P(g)$ to p_c is well described by the following law:

$$P(g) = p_c + Ag^a \tag{4}$$

where a is an exponent which characterizes the approach to the asymptotic threshold.

This property of convergence has been used to obtain a very accurate determination of the non-directed percolation threshold [13]. However, in the latter case, the correction exponent a is imply one [14].

Figure 2 shows a log–log plot of the difference $|P(g) - p_c|$ versus the gradient g for models A, B and C respectively. From this plot we can extract the values of a reported in table 1. The table summarizes the different numerical estimates of the scaling

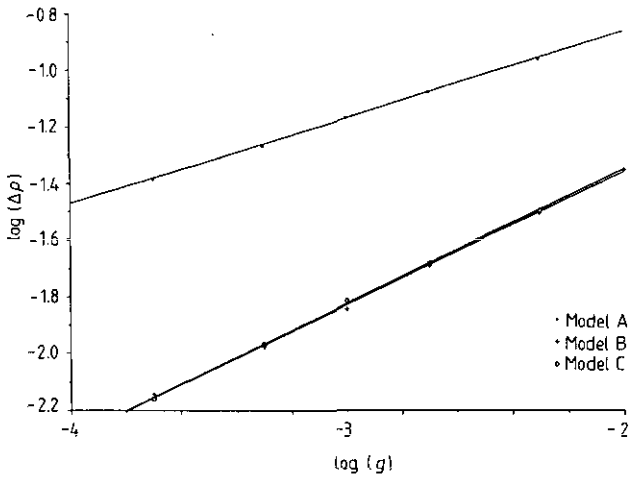

Figure 2. Log-log plot of the difference between the directed percolation threshold, p_c, and the mean position of the front, $P(g)$, as a function of the gradient g. Figures a, b and c refer respectively to models A, B and C.

Table 1.

Model	a	b	c
A	0.31	0.41	2.0
B	0.47	0.49	2.8
C	0.47	0.48	2.74
D	1	0.5	

exponents a, b and c in the four models studied in this article. For model D, the exponent a can assume different values according to the choice of the origin of probability. The presented derivation leads to $a \geqslant 2$ whereas the generic case is $a = 1$. This last result, which is the more meaningful is quoted in the table.

Using these estimates of the exponent a, we checked that the value of the threshold p_c obtained by fitting $P(g)$ versus g^a was consistent with the estimate used previously. In all cases A, B and C, we obtained $p_c = 0.6447 \pm 0.0001$.

For the Domany-Kinzel case, D, the threshold is known to be exactly $\frac{1}{2}$ [11]. We will show that the systematic deviation from this value obtained for a non-zero gradient is at most of the order g^2. Thus the exponent a is larger than or equal to two in this case. However, a difference that corresponds to less than a lattice spacing is not meaningful since it depends on the details of the discretization. Indeed, suppose we change the origin by one lattice spacing, then the mean position of the front is moved by $1/w = g$, introducing a correction term with an exponent $a = 1$. Therefore, in this model the generic exponent is $a = 1$, and the value $a \geqslant 2$ can be reached only for a very precise choice of the origin. In table 1, we report the generic value 1.

The width of the front z diverges for all cases when the gradient decreases. However, when translated in terms of probability, $\sigma(g) = gz$ goes to zero with g. More precisely the following dependence is observed:

$$\sigma(g) \propto g^b. \tag{5}$$

Figure 3 shows the log-log plot of $\sigma(g)$ versus g for cases A, B and C. The measured exponent is reported in table 1.

Both exponents a and b are needed to characterize the approach to p_c. One indicates the distance from the mean position of the front to the threshold, while the other gives the sharpening of the front. Large values of these exponents will be favourable to an accurate determination of the threshold when the latter is unknown. On the contrary, small values will go against this trend.

Generally, the width of the front is obtained [2, 3] by writing that at the extreme ends of the front, the correlation length, ξ, is equal to the distance to threshold. Using the divergence of ξ at threshold as

$$\xi \propto |p - p_c|^{-\nu} \tag{6}$$

one gets

$$\xi \propto (g\xi)^{-\nu}. \tag{7}$$

Hence, the width of the front expressed in lattice units is

$$\xi \propto g^{-\nu/(1+\nu)}. \tag{8}$$

When measured by the probability scale, the width of the front amounts to

$$\sigma(g) = g\xi \propto g^{1/(1+\nu)}. \tag{9}$$

Let us notice that ξ diverges when g tends to zero, but $\sigma(g)$ decreases to zero. The smaller the gradient, the steeper the front measured by the probability scale. This property is the basis of the determination of the threshold using a finite gradient [13, 14]. The scaling argument presented above is very general and has numerous applications for critical phenomena in an external field, or with a temporal or spatial variation of the control parameter. In experiments, the use of a gradient in the control parameter has also often been used to characterize precisely a critical threshold. The shift in the value of the threshold, as well as the smearing of the transition, are generally found to vanish critically as the gradient goes to zero as is the case in the examples we study here.

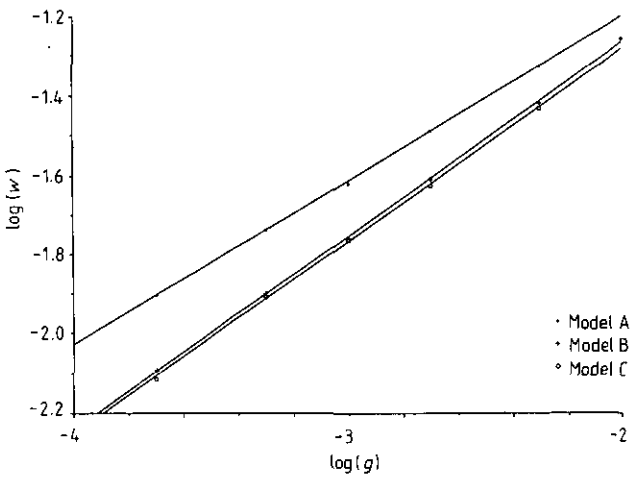

Figure 3. Log-log plot of the width of the front, $\sigma(g)$, as a function of the gradient g. Figures a, b and c refer respectively to models A, B and C.

In the case of directed percolation some care has to be taken to apply this argument. Two correlation lengths can be defined: one parallel to the preferred direction $\xi_\parallel$, and one perpendicular to it, $\xi_\perp$. Each one is characterized by a different critical exponent: $\nu_\parallel \approx 1.7334 \pm 0.0005$ and $\nu_\perp \approx 1.0972 \pm 0.0004$ [12].

For cases B and C, the gradient is orthogonal to the preferential direction, and thus we are led to use (8) with $\nu_\perp$, or

$$b = \frac{1}{(1+\nu_\perp)}. \tag{10}$$

Numerically, $b \approx 0.4768$ in good agreement with the estimates obtained in the simulations (see table 1). The fact that cases B and C give the same results is natural since their only difference is the way of probing the front. The clusters generated are identical in both cases.

For case A, the geometry is such that the expected result is

$$b = \frac{1}{(1+\nu_\parallel)} \tag{11}$$

or $b \approx 0.3658$. Numerically, this exponent is found to lie in between the two values (equations 10 and 11), with error bars that exclude both suggestions. Using the arithmetic mean, $\nu = (\nu_\parallel + \nu_\perp)/2$ gives a numerical value close to the measured exponent but we have no convincing argument to use such a combination.

Case D can be analysed exactly. The appendix gives the details of the computation for the whole profile of the front. Let us here simply consider the average height and width of the front. The front in each section is entirely determined by the position of the top site. Knowing this site in one section, i, the probability that the top site in the following section is j is given by a matrix element T_{ij} given in the appendix (equation A1). Let us consider that i is given. The mean value of $y(j)$ is

$$\langle y(j) \rangle = \sum_k T_{ik} y(k). \tag{12}$$

We consider the limit of a vanishing gradient g such that the product $y(i)g = q(x)$—which gives the position of the top site measured by the presence probability—is finite. The reason to impose such a limit is that we expect, according to the previously mentioned argument, that q, on average, will approach the threshold value. After some tedious but simple computations, we get

$$\langle q(x+1) \rangle = \langle qy(j) \rangle = q(x) + g\frac{(1-2q(x))}{(1-q(x))} - g^2\frac{(1-2q(x))}{(1-q(x))^3} + O(g^3). \tag{13}$$

The average position of the front, $P(g)$, is simply obtained by writing that $\langle q(x+1) \rangle = \langle q(x) \rangle = P(g)$ and solving (13) for $P(g)$. We obtain

$$P(g) = \tfrac{1}{2} + O(g^2). \tag{14}$$

Expressed in terms of probability, the average height of the front indeed converges towards the threshold, which for the Domany-Kinzel case is $\frac{1}{2}$. The correction term is analytic in g with an exponent larger than or equal to two. As mentioned previously, in the generic case, an exponent $a = 1$ is expected if the origin of probability is chosen differently by, say, one lattice constant.

As can be seen from (13), the fixed point of the transformation $P(g)$ is stable. Any perturbation from this value will decrease:

$$\langle q(x+1)\rangle - P(g) = (1-4g)(\langle q(x)\rangle - P(g)) + O(g^2). \tag{15}$$

Since the factor $(1-4g)$ is less than 1, the front is attracted toward its equilibrium value. This suggests the following analogy: the mean position of the front can be seen as a random walk in a potential well. It can be described by the Langevin equation:

$$\frac{\partial q(x)}{\partial x} = -\frac{dV(q)}{dq} + \eta(x) \tag{16}$$

where $V(q)$ is the potential, and η a Gaussian noise term. As previously, the x direction is along the mean direction of the front, whereas q is perpendicular to it. From (15) we deduce that at the first order in g is perpendicular to it. From (15) we deduce that at the first order in g the potential is harmonic, and can be written:

$$V(q) = 2g(q-\tfrac{1}{2})^2. \tag{17}$$

Naturally, in the limit of a zero gradient, we recover the analogy between the directed percolation problem and the random walk with no bias. The mean width of the front is such that $V(\frac{1}{2}+\sigma) = \text{constant}$ thus $\sigma \propto \sqrt{g}$ (or $b = \frac{1}{2}$). The appendix provides an exact derivation of the whole profile probability which will be shown to converge towards a Gaussian. As a consequence, σ can be computed exactly, and we will show that $\sigma = \sqrt{g}$ (with a unit prefactor).

In this case, the correlation length exponents are $\nu_\perp = 1$ and $\nu_\parallel = 2$. Thus we see that b satisfies (10) as expected from the relative orientation of D and G.

5. Jump size distribution

As mentioned in the introduction, Hensen *et al* [1] studied a case related to our problem. Namely, they studied directed site percolation in a gradient with a geometry similar to our case C. The key of their theoretical analysis lies on the notion of jump-size distribution. Let us recall their basic results:

When probing the front, the position of the top site jumps from one row to the next. The jumps will be the difference in height between two consecutive rows, $(h(x) = y(x) - y(x+1))$. Let us distinguish between the negative jumps, which correspond to a move of the front position away from the base line S, and positive jumps, which move towards S. On average the location of the front remains constant, close to the percolation threshold. Calling $n(h, g)$ the probability of having a jump h with a gradient g, we can write the balance equation:

$$\sum_{h<0} |h| n(h, g) = \sum_{h>0} h n(h, g) \tag{18}$$

for all values of g.

The dependence of $n(h, g)$ with h is very different when h is positive and when it is negative. Let us first consider negative jumps.

The simpler case is model C. In this case, the jumps cannot be smaller than -1, because of the orientation of the preferred direction. The probability of having $h = -1$ is simply $n_C(-1, g) = p_c(g)$. Thus we can rewrite (18) as

$$\sum_{h>0} h n_C(h, g) = p_c. \tag{19}$$

For models A and B, the conclusion is very similar, although the RHS of (19) is slightly more complicated. Indeed for model A the probability of having a negative h is $n_A(h, g) = p_c(g)(2-p_c(g))(1-p_c(g))p_c(g)^{h-1}$, whereas for model B it is $n_B(h, g) = (1-p_c(g))p_c(g)^h$. In both cases the distribution is exponential, and the sum $\Sigma\, hn(h, g)$ for negative h can be performed easily:

$$\sum_{h>0} hn_A(h, g) = (2-p_c)/(1-p_c)$$
$$\sum_{h>0} hn_B(h, g) = 1/(1-p_c). \tag{20}$$

In all cases, the first moment of positive jumps is finite and non-zero. Expanding this first moment for $p_c(g)$ close to p_c allows us to derive the leading correction term, and thus the exponent a. In order to do so, we need some more information about $n(h, g)$ for positive h. We again follow closely [1].

When no gradient is included in the model, i.e. $p = p_c$ everywhere in the lattice, the jump size distribution for positive h is a power-law

$$n(h) \propto h^{-c}. \tag{21}$$

A non-zero gradient introduces a cut-off in the distribution, which can then be written

$$n(h, g) = h^{-c}\phi(h, g^d) \tag{22}$$

where the function $\phi(x)$ is constant for $x \ll 1$, and converges to zero faster than any power law for $x \to +\infty$. The maximum jump, h_{max}, is thus of the order of g^{-d}. Hansen *et al* [1] propose to relate this cut-off to the width of the front

$$gh_{max} \propto \sigma \propto g^b \tag{23}$$

or $d = 1-b$. In [1], the exponent d was suggested to be $\nu_\perp/(1+\nu_\perp)$, in agreement with (10), for model C. However, the corresponding expected values for models A and B that we can deduce from this (cf. previous discussion) are not found.

The exponent c has been suggested [1] to be equal to $3-\beta/\nu_\perp$ for model C, where β is the critical exponent of the probability to belong to the infinite cluster $P_\infty \propto (p-p_c)^\beta$. In two dimensions, $\beta = 0.280 \pm 0.004$. The condition that the first moment is independent of g at the first order imposes that $c \geqslant 2$. Studying the directed site percolation problem in a gradient in higher space dimensions [12], Hansen *et al* reported that the distribution of jumps turned out not to be critical. In this case the distribution was a power-law with an exponent $c = 2$, up to logarithmic terms.

Hansen *et al* [1] concluded their analysis by using the expression of the jump size distribution in order to obtain the leading correction term to the mean position of the front. We have seen through (19) and (20), that the first moment of the positive jump size distribution was an analytic function of $p_c(g)$ for all cases considered. Expanding this function around p_c gives a correction to the first moment similar to the correction term for $p_c(g)$ itself. Different corrections terms can appear. As suggested in [1], the corrections are given by the singular parts of the first moment computed using the expression (22), i.e. $\Sigma\, hn(h, g) \approx \int h^{1-c}\phi(hg^d)\, dh|_{sing}$. The upper bound of this integral gives a singular term proportional to $g^{-d(2-c)}$, whereas the lower bound gives a term proportional to g^d. Considering these two possibilities, the leading correction exponent a is

$$a = \min(d, d(c-2)). \tag{24}$$

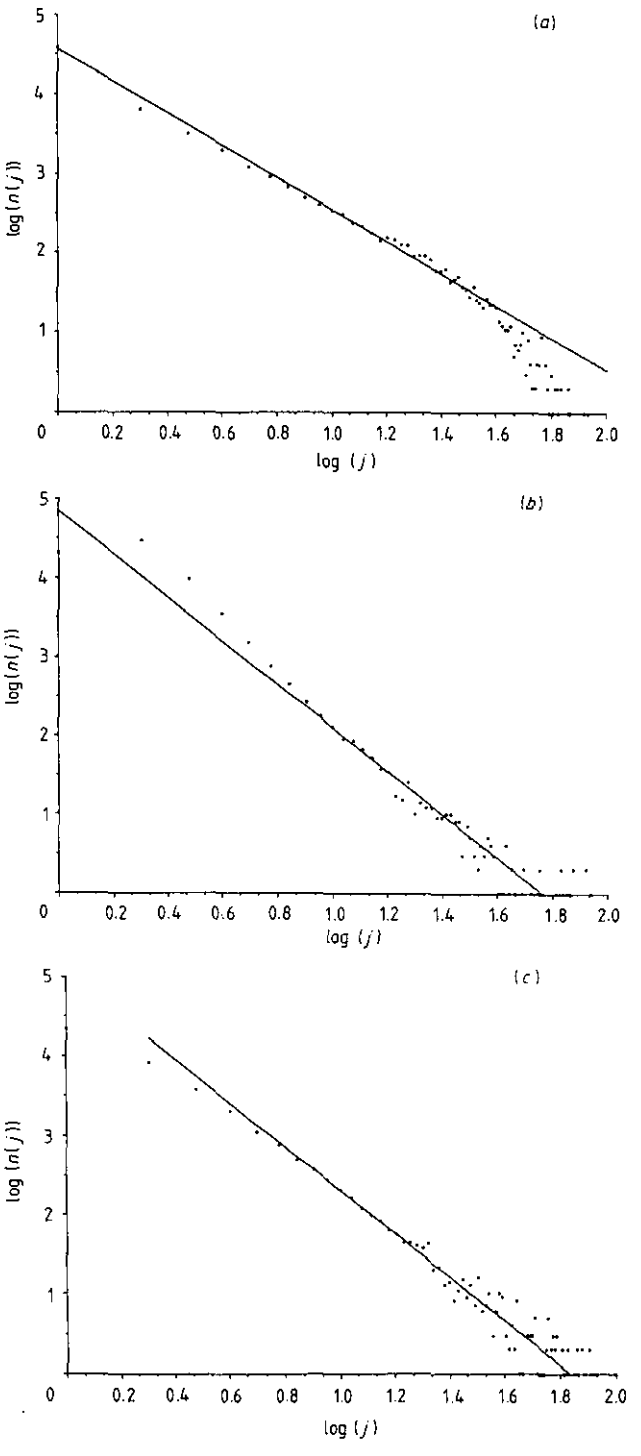

Figure 4. Log–log plot of the jump distribution $n(h)$ as a function of h, for a zero gradient, i.e. $p = p_c$ everywhere in the lattice. Figures a, b and c refer respectively to the orientations of D and T as in models A, B and C.

When $c<3$, the dominant correction is expected to be given by $a=d(c-2)$ otherwise, $a=d$. In the example studied by Hansen *et al* [1], it turned out that the leading correction term, i.e. the lower exponent, was hidden because of the small value of the prefactor of this term.

We have checked numerically the power-law distribution in all cases with no gradient. Figure 4(a-c) gives the log-log plot of this distribution for the three models. We observe a power-law behaviour with an exponent c respectively equal to 2.0, 2.8 and 2.74 as reported in table 1. We see a good agreement with the expected value for cases B and C, $3-\beta/\nu_\perp \approx 2.75$. For model A, it turns out that the exponent $c \approx 2$ is extremely close to the lower limit necessary to have the first moment convergent. It is interesting to note the analogy with the case of higher space dimensionalities considered by Hansen and Houlrik [15] where above an upper critical dimension, $c=2$.

We also checked that the presence of the gradient only generated a cut-off in the distribution, without altering the value of the exponent c. The scaling of the cut-off was found to be given by the width of the front itself, i.e. $d=1-b$.

In cases B and C, the agreement with the expected a exponent is reasonable since the dominant correction to scaling may be hidden due to the smallness of the first prefactor. The measured a exponent is 0.47, while the second expected value is $d=0.52$. For case A, however, the observed correction term is more singular than expected.

6. Conclusion

Despite the apparent simplicity of the problem, it appears that the scaling properties of the front geometrical characteristics are difficult to be account for. It would be extremely useful to be able to relate the measured exponents to known critical indices appearing in directed percolation.

The case of higher dimensions, investigated in [15] is amenable to a similar treatment. The sensitivity of the problem to the respective orientation of the gradient, the preferred direction and the probing direction would again be interesting in order to address the concrete problem of fronts in $2+1$ directions, i.e. the most common case. It would be also of interest to study cases out of equilibrium, such as an invasion percolation problem with a destabilizing gradient such as studied by de Arcangelis and Herrmann [16], in a different context.

Acknowledgments

We acknowledge numerous useful discussions with Alex Hansen.

Appendix

In this appendix we investigate analytically the shape of the front in the Domany-Kenzel limit (model D). As noted in the main text, the cluster will be compact since all bonds are present in one direction. Thus the front is uniquely determined in a section if we know the top site, say i. The probability T_{ij} that the front at the next section is located at a site j can easily be computed. If $j>i+1$, $T_{ij}=0$ since the front cannot jump by more than one lattice unit. If $j \leqslant i+1$, the leading to site j must be

present (probability $p(j)$) whereas all bonds starting from sites $k=j+1$ to $k=i$ must be absent (probability $1-p(k)$). Therefore the matrix element T_{ij} is equal to:

$$T_{ij} = p(j)((1-p(j+1))(1-p(1j+2))\ldots(1-p(i))) = \left(1-\frac{j}{n}\right)\frac{(i+1)!}{j!}\frac{1}{n^{i-j+1}}. \tag{A1}$$

We look for the probability density of the location of the front. Let us write ϖ_i the probability that the front site is at site i. The basis of the computation is to note that the vector ϖ_i is invariant when we go to the following section, or

$$\sum_i \varpi_i T_{ij} = \varpi_j. \tag{A2}$$

The vector ϖ is thus the eigenvector of the matrix $T^{\dagger}$ with the largest eigenvalue 1. Let us do the following change of variable:

$$a_i = \frac{(i+1)!}{n^{i+1}}\varpi_i. \tag{A3}$$

Equation (A2) now reads

$$\left(1-\frac{j}{n}\right)\left(\frac{j+1}{n}\right)\sum_{i=j-1}^{i=n} a_i = a_j. \tag{A4}$$

We introduce the sum $\Sigma_{i=j}^{i=n} a_i = b_j$ and rewrite (A4) as

$$\left(1-\frac{i}{n}\right)\left(\frac{i+1}{n}\right)b_{i-1} = b_i - b_{i+1}. \tag{A5}$$

The use of the ratio $c_j = b_j/b_{j-1}$ allows us to simplify the latter equation, and gives

$$\left(1-\frac{i}{n}\right)\left(\frac{i+1}{n}\right) = c_i(1-c_{i+1}). \tag{A6}$$

One sees from (A6) that $c_i = 1-i/n$ is a particular solution of the recurrence relation (A6). Since $c_n = b_n = a_n = 0$, this particular solution is the solution we look for. Introducing this expression in the definition of b_i gives

$$b_i = b_1\frac{n!}{(n-i-1)!\,n^i} \tag{A7}$$

and thus

$$a_i = b_1\frac{n!(i+1)}{(n-i-1)!\,n^{i+1}} \tag{A8}$$

and finally

$$\varpi_i = \binom{n}{i}(n-i)b_1. \tag{A9}$$

The normalization of the probability $\Sigma\,\varpi_i = 1$ determines the value of b_1. Using $\Sigma\binom{n}{i} = 2^n$ and $\Sigma\, i\binom{n}{i} = n2^{n-1}$, we obtain

$$b_1 = 1/(n2^{n-1}) \tag{A10}$$

and finally, we can write the probability vector

$$\varpi_i = \frac{2(n-i)}{n2^n}\binom{n}{i}. \tag{A11}$$

It is interesting to consider the large n limit, i.e. small gradient, with the requirement that the ratio $i/n = q$ is finite, as seen in the main text. Calling $g = 1/n$ the gradient of probability, and using Stirling formula, the probability ϖ_i can be written as

$$\varpi_i = 2\sqrt{\frac{g(1-q)}{2\pi q}}\,(2q^q(1-q)^{(1-q)})^{-1/g}. \tag{A12}$$

We introduce the continuum probability density $h(q)dq$ which gives the probability that the front height is between q and $q+dq$. We have $h(q) = \varpi_i/g$ for i such that $ig = q$

$$h(q) = 2\sqrt{\frac{(1-q)}{2\pi g q}}\,(2q^q(1-q)^{(1-q)})^{-1/g}. \tag{A13}$$

From (A13), we can compute the shape of the distribution in the vicinity of $q = \frac{1}{2}$. We obtain a Gaussian profile with a mean $\frac{1}{2}$ and a standard deviation equal to $\sqrt{g}$. Thus the exponent b is equal to $\frac{1}{2}$, as mentioned in table 1.

References

[1] Hansen A, Aukrust T, Houlrik J M and Webman I 1990 *J. Phys. A: Math. Gen.* **23** L143
[2] Sapoval B, Rosso M and Gouyet J-F 1985 *J. Physique Lett.* **46** L149
[3] Rosso M, Gouyet J-F and Sapoval B 1986 *Phys. Rev. Lett.* **57** 3195; 1988 *Phys. Rev.* B **37** 1832
[4] Meakin P, Ramanlal P, Sander L M and Ball R C 1986 *Phys. Rev.* A **34** 5091
[5] Meakin P and Jullien R 1987 *J. Physique* **48** 1651
[6] Jullien R and Meakin P 1987 *Europhys. Lett.* **4** 1385
[7] Zabolitzky J G and Stauffer D 1986 *Phys. Rev.* A **34** 1523
[8] Meakin P, Botet R and Jullien R 1986 *Europhys. Lett.* **1** 609
[9] Kardar M, Parisi G and Zhang Y C 1986 *Phys. Rev. Lett.* **56** 889
[10] Nadal J P Thèse de troisième cycle (Paris)
[11] Domany E and Kinzel W 1981 *Phys. Rev. Lett.* **47** 5
[12] Essam, J W, De'Bell K, Adler J and Bhatti F M 1986 *Phys. Rev.* B **33** 1982
[13] Ziff R M and Sapoval B 1986 *J. Phys. A: Math. Gen.* **19** L1169
[14] Rosso M, Gouyet J-F and Sapoval B 1985 *Phys. Rev.* B **32** 6053
[15] Hansen A and Houlrik J M 1990 *Preprint*
[16] Arcangelis J de and Herrmann H J 1990 *J. Phys. A: Math. Gen.* **23** L923, (90)